

Response quantity of interest

The response quantity of interest in the present analysis is the maximum impact force experienced by the spacer grids (SG) in model #3 during the seismic event. Distinction is made between fuel assemblies at control assembly positions (CA) and non-control assembly positions (non-CA). For the success of control rod insertion, the fuel assemblies at control assembly positions are relevant. For each ground motion record, a total of six impact force data are evaluated given in Table 2.

Table 2: Quantities of interest – maximum of spacer grid impact forces in the core

	All SG at CA positions	All SG at non-CA positions	All SG
Load case 15	F _{15,CA}	F _{15,Non-CA}	F _{15,tot}
Load case 24	F _{24,CA}	F _{24,Non-CA}	F _{24,tot}

CORRELATION ANALYSIS

Correlation between ground motion intensity measures

Figure 3 shows the estimates of the correlation coefficients between pairs of quantities ξ, η

$$\rho_{\xi\eta} = \frac{E[(\xi - \mu_{\xi})(\eta - \mu_{\eta})]}{\sigma_{\xi}\sigma_{\eta}} \quad (1)$$

where μ_{ξ} and μ_{η} are the mean values and σ_{ξ} and σ_{η} are the standard deviations of ξ and η . Intense red and blue colours indicate high positive and negative correlations, respectively.

Several observations can be made with the colour map of the correlations:

There are two groups of intensity measures where the group members exhibit a strong positive correlation. These two groups are clearly visible in the correlation map, in the form of two large red squares. The two groups include the following intensity measures:

- Group 1: peak ground acceleration, velocity and displacement (PGA, PGV, PGD); cumulative absolute velocity (CAV) and Arias intensity (I_A)
- Group 2: T_5, T_{75}, T_{95} (time at which 5%, 75% and 95% of the I_A are reached); T_{US} (strong motion duration used in the US, $T_{75}-T_5$), T_F (strong motion duration used in France, $T_{95}-T_5$)

The remaining intensity measures are on one hand the average number of (upward) zero crossings (v_0) and maxima (v_1), per unit time, respectively. These form a group of strong mutual correlation. However, they can be also viewed as members of an “extended Group 2”, because a clear negative correlation pattern with the members of Group 2 is visible. This pattern is represented by the blue rectangles to the right and below the “Group 2 square”.

Finally, the average peak factors E_{peak} (one for each direction) essentially form a group by themselves.

Within the groups of intensity measures, there is significant correlation between the different directions (e.g. PGA_x, PGA_y and PGA_z). The cross-direction correlation is somewhat lower for the PGD.

Correlation between ground motion intensity measures and impact forces

Figure 3 can be further inspected for the correlation between the intensity measures and the effects of the ground motion on the FA, more specifically on the maximum impact forces (recall Table 2). The corresponding columns of the correlation matrix are the six rightmost columns in Figure 3.

The correlation map clearly indicates there is a strong positive correlation between the peak ground accelerations, velocities and displacement and the maximum impact forces. In contrast, there is very little correlation between the Group 2 intensity measures (duration) and the impact forces.

The two intensity measures for which there is the strongest correlation with the maximum impact forces (around 90%) are the PGV (load case 15) and the Arias Intensity (load case 24).

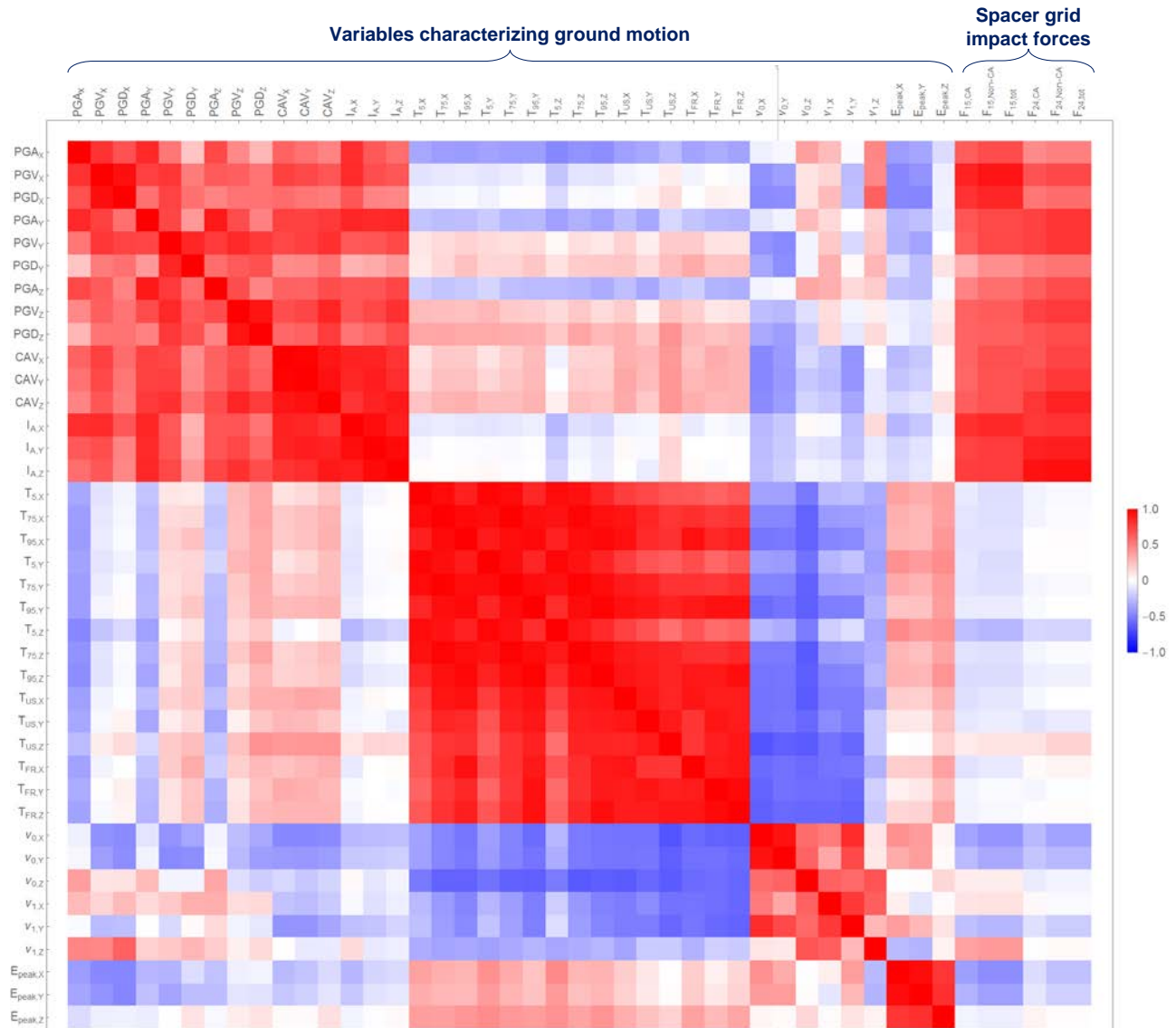


Figure 3: Colour map of the correlation matrix between intensity measure variables and impact forces

Linear regression in log-space

The maximum impact force $F_{15,tot}$ is plotted versus the PGV (X-direction) in Figure 4 below. Linear regression was applied in log-space, as described by Zentner et al. (2017),

$$\ln Y = \ln b + c \ln \alpha + \sigma \varepsilon \quad (2)$$

In this case, Y represents the maximum impact force of a given time history, α represents the used intensity measure. The parameters b and c define the regression line, σ defines the standard deviation and ε is a standard normal random variable.

There are several ground motion records for which no impacts occur at all. These samples are plotted in red colour in Figure 4. Obviously these data cannot be used in determining the regression parameters, which are hence exclusively based on the data plotted in black.

The upper limit of the range of the vertical axis is given by the buckling strength. The results show that large margins exist, even for the two extreme events (records 15903 and 103).

It is important to keep in mind that the variability represented by σ - and hence by the $\pm\sigma$ uncertainty band in the regression diagram - is entirely due to the ground motion variability. Indeed, the 28 ground motion records are propagated through the same model. No simultaneous sampling of model parameters, such as stiffness or damping of ground, building or components, is performed. Using the fragility terminology, the epistemic uncertainties associated with the analysis models are not included in the data shown in Figure 4.

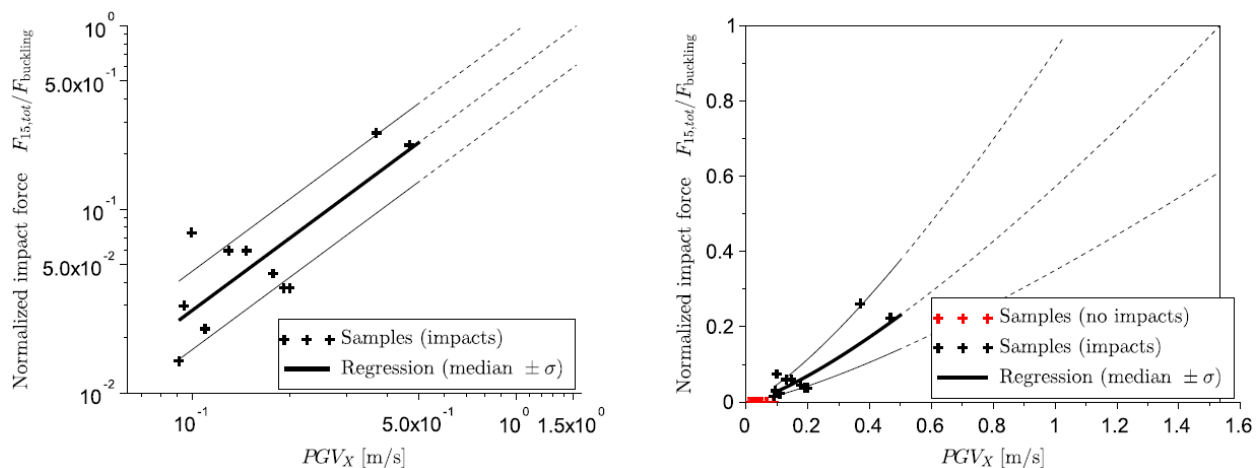


Figure 4: Maximum impact force $F_{15,tot}$ (normalized with respect to buckling resistance) vs. PGV_X, logarithmic axes (left) and linear axes (right)

SCALING OF INPUT EXCITATION (FUEL ASSEMBLY ROW MODEL)

For each of the 28 ground motion records, the last step of the analysis cascade in Figure 1, that is the fuel assembly row model, is repeated with amplified input excitation. More specifically, the input excitation is amplified by a scaling factor of 2, 4 and 8, respectively. The purpose of this analysis is twofold. Firstly, it is possible to estimate for which scaling factor the maximum impact force reaches the buckling resistance of the spacer grids. Secondly, it provides insight as to whether the maximum impact force is somewhat proportional to the amplitude of the input excitation.

The results of this analysis are shown in Figure 5. Two curves are shown for each of the 28 ground motion records, one for each horizontal direction. In addition, Figure 5 shows the same results for the two time histories that are representative of the 50% and the 84%-fractile of the floor response spectra based on the uniform hazard spectra (UHS) for $10^{-4}/a$. Several observations are suggested by the data:

1. The impact forces indeed scale more or less linearly with the amplitude of the input excitation. It is reiterated that in this analysis only the last step of the analysis cascade is repeated. Hence, the term input excitation refers to the motion of the upper and lower supports of the fuel assemblies in this case.
2. For all ground motion records, the maximum impact forces remain below the buckling resistance of the spacer grid if the fuel assembly input excitation is scaled by a factor of four or less. For almost all ground motion records, the maximum impact forces remain below the buckling resistance even if the fuel assembly input excitation is scaled by a factor of eight. An exception is represented by the two “outliers” in Figure 4 (records 15903 and 103). For record 1590, the impact force exceeds the buckling resistance for a scaling factor below eight for both horizontal directions; for record 103 this is the case only for the horizontal direction Y (load case “24”). It is noted that for the outlier records 15903 and 103, the permanent deformation resulting for a scaling factor of eight has been evaluated and found to be still in the admissible range.
3. The variability of the maximum impact forces is mainly driven by ground motion variability. This is suggested by the fact that the maximum impact forces corresponding to the 50% and 84%-fractiles of the UHS floor response spectra are relatively close to each other. The variability of the UHS is entirely due to the epistemic uncertainty of the soil-structure interaction model (damping and stiffness of soil and reactor building). This variability obviously translates to a smaller variability of the impact forces, compared to the ground motion variability, reflected by the curves corresponding to the 28 ground motion records.
4. The impact forces corresponding to the UHS excitations are enveloping the vast majority of the ground motion records, mostly by a large amount. Exceptions are the above-mentioned outliers. This is in line with the comparison of floor response spectra performed by Stäuble-Akçay et al. (2018).

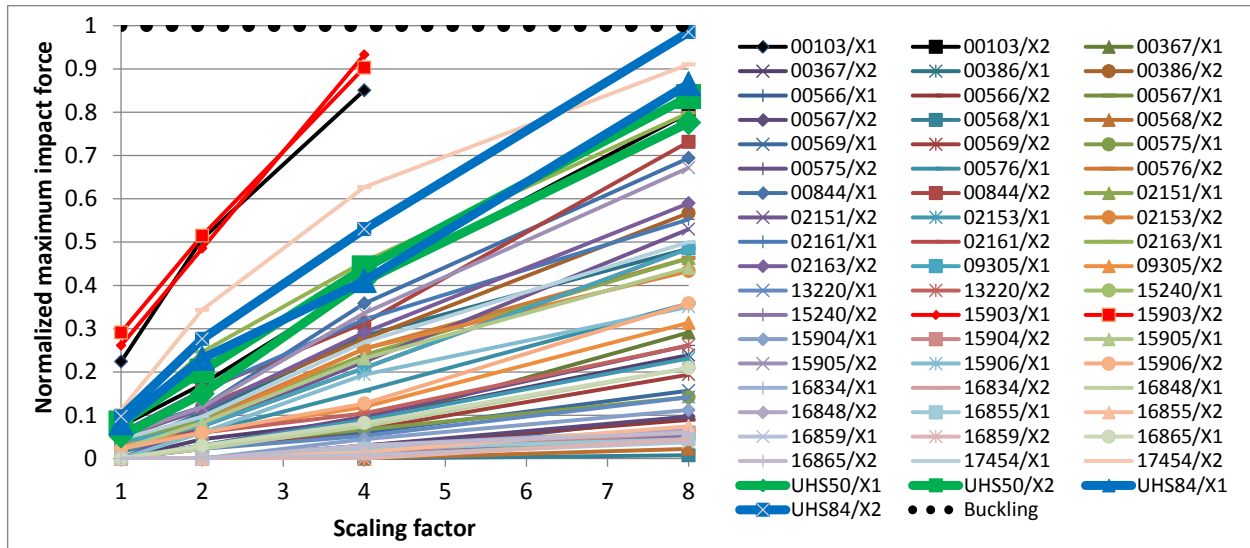


Figure 5: Maximum impact force versus scaling factor applied to the input excitation of the fuel assembly row model

CONCLUSIONS

Framatome had successfully performed demonstrations of safe control rod insertion for Goesgen even in case of permanent spacer grid deformations resulting from increased seismic hazard ENSI-2015. These demonstrations were based on ground motion time histories compatible with uniform hazard spectra (UHS) corresponding to a frequency of exceedance of $10^{-4}/a$.

In the present paper, the seismic performance of fuel assembly rows is analysed for historical ground motion records of seismic events in Europe that are compatible with the seismic hazard background of Goesgen NPP, at the same frequency of exceedance of $10^{-4}/a$. The resulting maximum impact forces between fuel assembly spacer grids show that there are ample margins with respect to the buckling resistance of the spacer grids. Hence the buckling resistance can be used as a more conservative criterion.

The correlation analysis of the ground motion intensity measures and the impact forces shows that there are two groups of strongly correlated intensity measures: one including the peak ground accelerations, velocities, displacements, the CAV and the Arias intensities; the other one including the parameters relevant for the duration. The impact forces strongly correlate with the first group, in particular with the PGV and the Arias intensity. This is reflected by the linear regression (in log-space) of the impact forces on an individual intensity measure.

Amplification of the input excitation of the fuel assembly row model by scaling factors 2, 4 and 8 is performed. The maximum impact forces scale more or less linearly with the amplification factor. The application of the scaling factors confirms the large margins: For all considered ground motion records, the maximum impact forces remain below the buckling resistance of the spacer grids even if the input excitation is scaled by a factor of 4. Furthermore, the allowable deformation is not exceeded even if the input excitation is scaled by a factor of 8.

The results also show that the impact forces corresponding to UHS are significantly larger than those resulting from most of the selected ground motion records.

Finally, it is remarked that the variability of the maximum impact forces is mainly driven by ground motion variability. In comparison, the effect of the epistemic uncertainty associated with the soil-structure interaction model is marginal.

The presented analysis of fuel assembly performance for recorded ground motion at Goesgen is a novel approach that is pursued by Framatome in order to add realism to the safety evaluation of fuel assemblies and identify additional, previously unquantified, margins at plants with challenging seismic conditions.

NOMENCLATURE

CAV	Cumulative Absolute Velocity, $CAV = \int_0^T a(t) dt$
I_A	Arias Intensity, $I_A = \frac{\pi}{2g} \int_0^T a(t)^2 dt$
PGA	Peak Ground Acceleration
PGD	Peak Ground Displacement
PGV	Peak Ground Velocity
v_0	Average number of (upward) zero crossings per unit time
v_1	Average number of maxima per unit time

HTP is a trademark or a registered trademark of Framatome or its affiliates, in the USA or other countries.

REFERENCES

- EMSC, European-Mediterranean Seismological Centre, 2013, “RESORCE Reference Database for Seismic Ground-Motion in Europe”, EMSC France
- Hilpert, R., et al. (2019). “Nonlinear Finite Element Analysis of Seismic Loads on RPV Internals” *SMiRT-25*, Charlotte, NC, USA, August 4-9, 2019.
- Pellisetti, M., Nykyforchyn, A., Rangelow, P., Schramm, K., Keßler, H., Klügel, J.-U., Klapp, U. (2015). “Seismic robustness of reactor trip via control rod insertion at increased seismic hazard estimates” *SMiRT-23*, Manchester, UK, August 10-14, 2015.
- Pellisetti, M., Keßler, H., Laudarin, F., Altieri, D., Nykyforchyn, A., Patelli, E., Klügel, J.-U. (2017). “Statistical analysis of impact forces and permanent deformations of fuel assembly spacer grids in the context of seismic fragility” *SMiRT-25*, Manchester, UK, August 20-25, 2017.
- Stäuble-Akcay, S., et al. (2018). “Seismic safety reassessment of NPP Goesgen after completion of site-specific probabilistic seismic hazard analysis” *16th European Conference on Earthquake Engineering*, Thessaloniki, Greece, June 18-21, 2018.